

## Accepted Manuscript

Synthesis of 1-benzyl-1H-benzimidazoles as galectin-1 mediated anticancer agents

Nerella Sridhar Goud, S. Mohammad. Ghouse, Jatoth Vishnu, D. Komal, Venu Talla, Ravi Alvala, Jakkula Pranay, Janish Kumar, Insaf A. Qureshi, Mallika Alvala

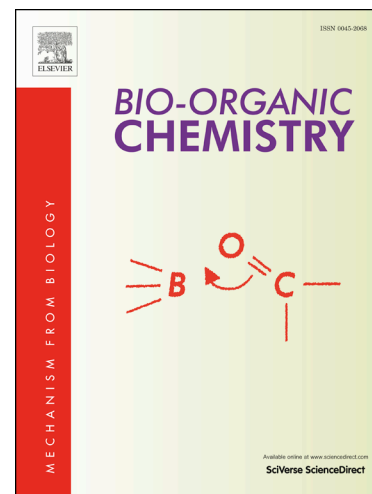
PII: S0045-2068(18)30681-3  
DOI: <https://doi.org/10.1016/j.bioorg.2019.103016>  
Article Number: 103016  
Reference: YBIOO 103016

To appear in: *Bioorganic Chemistry*

Received Date: 9 July 2018  
Revised Date: 7 May 2019  
Accepted Date: 26 May 2019

Please cite this article as: N. Sridhar Goud, S. Mohammad. Ghouse, J. Vishnu, D. Komal, V. Talla, R. Alvala, J. Pranay, J. Kumar, I.A. Qureshi, M. Alvala, Synthesis of 1-benzyl-1H-benzimidazoles as galectin-1 mediated anticancer agents, *Bioorganic Chemistry* (2019), doi: <https://doi.org/10.1016/j.bioorg.2019.103016>

This is a PDF file of an unedited manuscript that has been accepted for publication. As a service to our customers we are providing this early version of the manuscript. The manuscript will undergo copyediting, typesetting, and review of the resulting proof before it is published in its final form. Please note that during the production process errors may be discovered which could affect the content, and all legal disclaimers that apply to the journal pertain.



## Synthesis of 1-benzyl-1H-benzimidazoles as galectin-1 mediated anticancer agents

Nerella Sridhar Goud <sup>a</sup>, S. Mahammad. Ghouse <sup>a</sup>, Jatoth Vishnu <sup>b</sup>, D. Komal <sup>a</sup>, Venu Talla <sup>b</sup>, Ravi Alvala <sup>c</sup>, Jakkula Pranay <sup>d</sup>, Janish Kumar <sup>d</sup>, Insaf A. Qureshi <sup>d</sup>, Mallika Alvala <sup>a\*</sup>

<sup>a</sup> Department of Medicinal Chemistry, National Institute of Pharmaceutical Education and Research (NIPER), Hyderabad 500 037, India

<sup>b</sup> Department of Pharmacology and Toxicology, National Institute of Pharmaceutical Education and Research (NIPER), Hyderabad 500 037, India

<sup>c</sup> G. Pulla Reddy College of Pharmacy, Hyderabad 500 028, India.

<sup>d</sup> Department of Biotechnology & Bioinformatics, School of Life Sciences, University of Hyderabad, Hyderabad-500046, India.

### ABSTRACT

In our pursuit to develop novel non-carbohydrate small molecule Galectin-1 Inhibitors, we have designed a series of 1-benzyl-1H-benzimidazole derivatives and demonstrated their anticancer activity. The compound **6g**, 4-(1-benzyl-5-chloro-1H-benzo[d]imidazol-2-yl)-N-(4-hydroxyphenyl) benzamide was found to be most potent with an IC<sub>50</sub> of 7.01 ± 0.20 μM and arresting MCF-7 cell growth at G2/M phase and S phase. Induction of apoptosis was confirmed by morphological changes like cell shrinkage, blebbing and cell wall deformation, dose dependent increase in the mitochondrial membrane potential (ΔΨ<sub>m</sub>) and ROS levels. Further, dose dependent decrease in Gal-1 protein levels proves Gal-1 mediated apoptosis by **6g**. Molecular docking studies were performed to understand the Gal-1 interaction with compound **6g**. In addition, RP-HPLC studies showed 85.44% of **6g** binding to Gal-1. Binding affinity studies by fluorescence spectroscopy and Surface Plasmon Resonance (SPR) showed that **6g** binds to Gal-1 with binding constant (K<sub>a</sub>) of 1.2x10<sup>4</sup> M<sup>-1</sup> and equilibrium constant KD value of 5.76 x10<sup>-4</sup> M respectively.

### Research Highlights

- Series of small molecules 1-benzyl-1H-benzimidazole analogues were synthesized.
- Identified the synthetic molecule **6g** which lowers the Gal-1 expression in MCF-7 cells.
- Reporting **6g** as anticancer agent with an  $IC_{50}$  of  $7.01 \pm 0.20 \mu\text{M}$  mediated by Gal-1.
- Reporting the binding studies by SPR and fluorescence spectroscopy of non-carbohydrate compound **6g** to Gal-1.

**Key words:** 1-benzyl-1H-benzimidazoles, Galectin-1, cancer, Fluorescence Spectroscopy, RP-HPLC, Surface Plasmon Resonance.

## 1. Introduction

Human Galectin-1 (Gal-1) is a family of carbohydrate-binding protein of S-type (abundance in cysteine residues/ sulfhydryl residues) lectin having a high affinity for  $\beta$ -galactosides on the cell surface and extracellular glycoproteins and on glycolipids. Gal-1 is located both extracellularly and intracellularly and found at the cell surface as secreted Gal-1 binds to lactosamines on glycoconjugates expressed by the same cell or by neighbouring cells. Gal-1 is expressed differentially by various normal and pathological tissues and appears to be functionally multivalent, undertaking a wide range of biological activity [1]. Reports from various studies show that Gal-1 contributes in tumour metastasis, cell adhesion, increased invasiveness, angiogenesis and evasion of the immune response. Gal-1 plays a key role in adhesion of prostate and ovarian cancer cells to the Extra Cellular Matrix (ECM) and in turn mediates cancer progression [2, 3], also mediate homotypic cell aggregation of human melanoma cells in a carbohydrate-dependent manner and, it has been shown to affect cell migration of cancer cells and influence their invasiveness [4]. Recombinant Gal-1 added extracellularly to melanoma cells induces a dose dependent increase in cell-adhesion to laminin or fibronectin [5]. In fact,

exogenously added Gal-1 causes increased motility of glioblastoma cells *in vitro* [6]. Gal-1 induces cell growth inhibition in human T-cells, inhibits T-cell activation and promotes apoptosis of activated T cells [7]. Furthermore, *Matarrese et al.* showed that Gal-1 sensitises resting T cells to CD95/Fas-mediated cell death [8]. Intracellular Gal-1 plays a key role in the initiation of transformed phenotype of tumours via interacting with signalling pathways such as p21 [9], ganglioside GM1 receptor related pathways [10], RAS [11], RAF and PI3/K [4]. It has been proven that Gal-1 is over expressed in pancreatic ductal adenocarcinomas as compared to normal tissue and pancreatitis [12]. Tumour cells may impair T-cell effector functions through secretion of Gal-1 and this mechanism may contribute in tilting the balance towards an immunosuppressive environment at the tumour site. The link between Gal-1 mediated immune regulation and its contribution to tumour-immune escape has been well established through various knock down transfectant experiments. Blanchard H *et al.* summarized about **monovalent- and multivalent-carbohydrate-based inhibitors, peptides- and peptidomimetics as Gal-1 inhibitors** and their potential therapeutic applications in their patent review [13]. Current study was initiated with an aim to develop non carbohydrate Gal-1 inhibitors as anticancer agents.

Benzimidazole (1H-benzo[d]imidazole) is a privileged scaffold, due to its presence in a wide range of bioactive compounds by interacting with numerous biomolecular targets and exhibit diverse activities like Antihypertensive [14], Anti-inflammatory [15], Antimicrobial [16], Antiviral [17], Antiparasitic [18], Antioxidants [19], Anticoagulants [20], CNS stimulants [21] and anticancer activity [22]. The research in the development of bioactive molecules with benzimidazole nucleus has accelerated during last 10 years hence it has substantially been used as a lead compound to design and synthesize analogues with improved activity. Bendamustine is a US FDA approved anti-cancer drug

containing benzimidazole moiety (**Figure-1**). Telmisartan possessing an N-benzylated benzimidazole moiety is reported to induce early apoptosis in the prostate cancer cells [23]. *Tsung-Chieh Shih et al.* reported a novel Gal-1 inhibitor named LLS2 which was discovered through One-Bead-Two Compound library and potentiated the anti-tumour effects of Paclitaxel *in vivo* [24]. The same group reported another novel Gal-1 inhibitor named LLS30 which showed synergistic anti-tumor activity with docetaxel and also effectively inhibit the metastasis and invasion of prostate cancer *in vivo* [25].

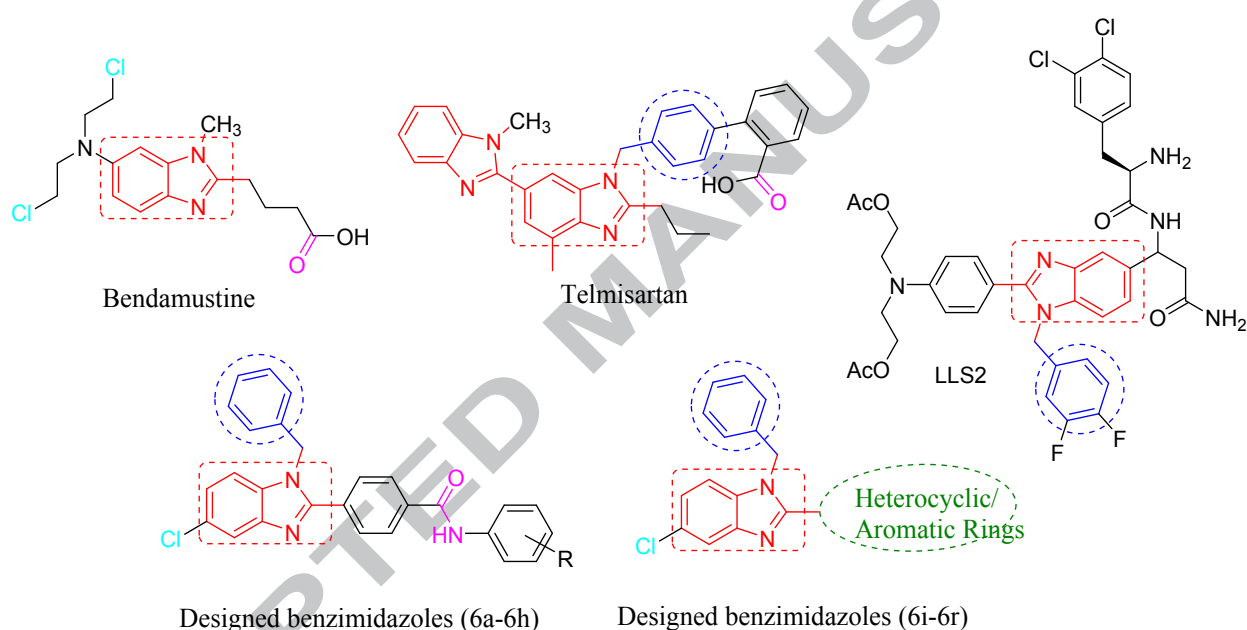


**Figure 1.** Representative examples of available benzimidazole drugs, reported derivatives and rationale for the designed target compounds **6a-6r**.

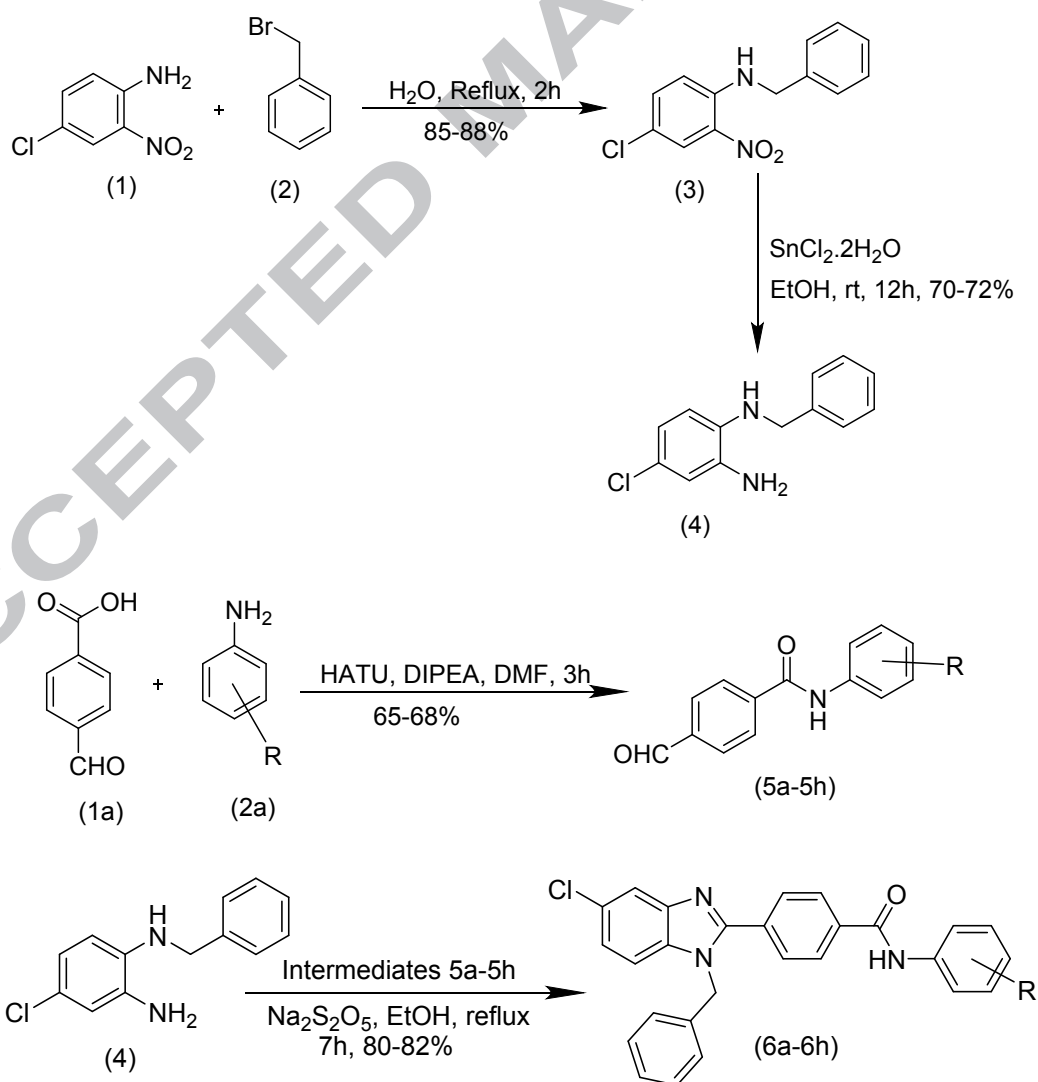
With our interest to develop more potent cytotoxic molecules via Gal-1 inhibition, the present study aims in synthesis of non-carbohydrate small molecules 1-benzyl-1H-benzimidazoles.

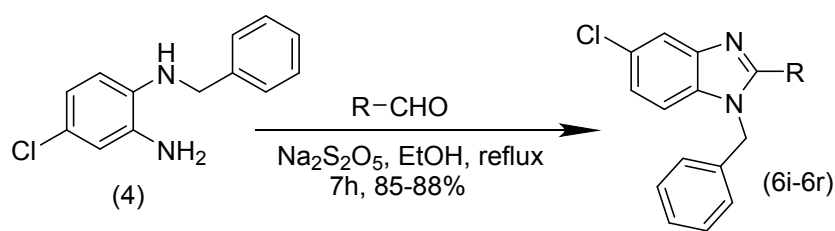
## 2. Results and Discussion

### 2.1. Chemistry

The synthetic strategy for the preparation of 1-benzyl-1H-benzimidazole analogues **6a-6r** is shown in **Scheme-1**. The N1-benzyl-4-chlorobenzene-1,2-diamine (**4**) was condensed with various 4-formyl-N-phenylbenzamides (**5a-**

**5h**), various aromatic and heterocyclic aldehydes. Initially the N-benzyl-4-chloro-2-nitroaniline (**3**) was synthesized from commercially available 4-chloro-2-nitro aniline with benzyl bromide [26] and the nitro group of compound (**3**) was further reduced to amino functional group by using stannous chloride dihydrate offered N<sup>1</sup>-benzyl-4-chlorobenzene-1,2-diamine (**4**). On the other hand, the 4-formyl-N-phenylbenzamides (**5a-5h**) were synthesized from the commercially available 4-formyl benzoic acid and different aniline derivatives [27]. Finally, refluxing 4-formyl-N-phenylbenzamides (**5a-5h**), different aromatic and heterocyclic aldehydes and N<sup>1</sup>-benzyl-4-chloro orthophenylene diamine in ethanol in the presence of sodium metabisulphite [28] furnishing the target compounds **6a-6r** with moderate to good yields.





- |   |  |
|---|--|
| <b>6a</b> R = H                                   | <b>6i</b> R = indole-3-yl                      |
| <b>6b</b> R = 4-OCH <sub>3</sub>                  | <b>6j</b> R = pyrrole-2-yl                     |
| <b>6c</b> R = 4-CH(CH <sub>3</sub> ) <sub>2</sub> | <b>6k</b> R = benzo[d][1,3]dioxole-5-yl        |
| <b>6d</b> R = 4-F                                 | <b>6l</b> R = furan-2-yl                       |
| <b>6e</b> R = 3,4,5-tri-OCH <sub>3</sub>          | <b>6m</b> R = pyridine-2-yl                    |
| <b>6f</b> R = 3,4,5-tri-CH <sub>3</sub>           | <b>6n</b> R = thiophene-2-yl                   |
| <b>6g</b> R = 4-OH                                | <b>6o</b> R = 8-hydroxyquinolin-2-yl           |
| <b>6h</b> R = 4-Cl                                | <b>6p</b> R = 3-phenoxyphen-1-yl               |
|   | <b>6q</b> R = 3-ethoxy-4-hydroxyphen-1-yl      |
|   | <b>6r</b> R = 3,5-dimethoxy-4-hydroxyphen-1-yl |

**Scheme 1.** Synthesis of different 1-benzyl-1H-benzimidazole analogues **6a-6r**.

All synthesized compounds (**6a-6r**) were characterized by analytical techniques viz. HRMS, <sup>1</sup>H and <sup>13</sup>C-NMR Spectroscopy. The <sup>1</sup>H-NMR spectrum of **6a** showed a sharp singlet of CH<sub>2</sub> protons of benzyl group at δ 5.60 and a sharp singlet of N-attached proton (amidic proton) at δ 10.45 and remaining all protons appeared in the range of δ 6.90-8.45. In the <sup>13</sup>C-NMR spectrum of **6a**, the N-attached methylene carbon of benzyl group appeared at δ 48.22 and the carbonyl carbon appeared at δ 165.21. The remaining all carbons appeared in the range of δ 113.29-154.19. Similar fashion was observed in the <sup>1</sup>H-NMR and <sup>13</sup>C-NMR spectra of all other compounds (**6a-6r**). The HRMS (ESI) of **6a-6r** showed corresponding [M+H]<sup>+</sup> peaks based on their molecular weights.

## 2.2. Biological Activity

### 2.2.1. In vitro cytotoxic activity

The synthesized 1-benzyl-1H-benzimidazole derivatives (**6a-6r**) were screened for their *in vitro* cytotoxicity against a panel of human cancer cell lines viz. Lung cancer (A-549), prostate cancer (DU-145), breast cancer (MCF-7 and MDA-MB-231) and colorectal cancer (HCT-116 and HT-29), using 3-(4,5-dimethylthiazol-2-yl)-2,5-diphenyltetrazolium bromide (MTT) assay [29]. The IC<sub>50</sub> (μM) values of compounds **6a-6r** and the standard, 5-fluorouracil are displayed in **Table-1**.

**Table 1.** IC<sub>50</sub> (μM) values<sup>a</sup> for the derivatives 6a-6r by MTT assay.

Compound	A-549 <sup>b</sup>	DU-145 <sup>c</sup>	MCF-7 <sup>d</sup>	MDA-MB-231 <sup>d</sup>	HCT-116 <sup>e</sup>	HT-29 <sup>f</sup>
6a	12.14 ± 0.21	>15	10.03 ± 0.50	>15	14.32 ± 0.37	>15
6b	>15	>15	11.81 ± 0.75	>15	>15	>15
6c	12.84 ± 0.32	>15	10.09 ± 0.51	>15	>15	>15
6d	>15	>15	11.52 ± 0.45	>15	>15	14.12 ± 0.55
6e	>15	>15	>15	>15	>15	13.39 ± 0.21
6f	>15	>15	9.30 ± 0.42	>15	>15	>15
6g	10.69 ± 0.14	13.89 ± 0.74	7.01 ± 0.20	14.04 ± 0.62	12.91 ± 0.52	37.86 ± 0.42
6h	>15	>15	>15	9.61 ± 0.24	>15	>15
6i	>15	>15	>15	>15	>15	>15
6j	>15	>15	7.29 ± 0.71	>15	>15	>15
6k	>15	>15	>15	>15	>15	>15
6l	>15	>15	>15	>15	>15	>15
6m	>15	>15	>15	>15	>15	>15
6n	>15	>15	>15	>15	>15	>15
6o	>15	>15	>15	>15	11.84 ± 0.82	>15
6p	13.46 ± 0.17	>15	11.63 ± 0.24	>15	>15	>15
6q	>15	>15	7.50 ± 0.83	>15	>15	>15
6r	>15	>15	7.14 ± 0.70	>15	>15	>15
5-fluorouracil	1.60 ± 0.10	1.92 ± 0.16	3.20 ± 0.50	0.60 ± 0.30	1.16 ± 0.06	3.90 ± 1.10

<sup>a</sup>50% Inhibitory concentration after 48 hr of drug treatment. <sup>b</sup> Human lung cancer. <sup>c</sup> Human prostate cancer. <sup>d</sup> Human breast cancer. <sup>e, f</sup> Human colorectal cancer.

Among all, the compound **6g** had shown significant growth inhibition with an  $IC_{50}$  of  $10.69 \pm 0.14 \mu\text{M}$ ,  $13.89 \pm 0.74 \mu\text{M}$ ,  $7.01 \pm 0.20 \mu\text{M}$ ,  $14.04 \pm 0.62 \mu\text{M}$ ,  $12.91 \pm 0.52 \mu\text{M}$  in A-549, DU-145, MCF-7, MDA-MB-231 and HCT-116 cell lines, respectively with 7.73% inhibition on Normal Rattus Norvegicus Kidney (NRK) cells at  $20 \mu\text{M}$  concentration. The compound **6g** displayed no cytotoxicity against NRK-52E (normal kidney cells) and L-132 (normal lung cells) with an  $IC_{50}$  values of  $126.45 \mu\text{M}$  and  $220.56 \mu\text{M}$  respectively, which clearly indicates that the compound is nontoxic. Further mechanistic studies of **6g** were carried in MCF-7 cell line at 1.25, 2.5, 5 and  $10 \mu\text{M}$  concentrations.

### 2.2.2. Acridine Orange/Ethidium Bromide (AO/EB) staining

Acridine Orange (AO)/Ethidium Bromide (EB) staining assay is performed to differentiate between live, apoptotic and necrotic cells [30]. Acridine Orange (AO) can permeate the intact cell membrane and stain the nuclei green, whereas Ethidium Bromide (EB) can only stain the nucleus of cells that have lost membrane integrity in red. It can be inferred from **Figure 2** that the control cells display normal morphology and appeared green in colour. Fluorescence microscopic images of MCF-7 cells treated with compound **6g** clearly showed morphological changes such as membrane blebbing, cell shrinkage, chromatin condensation and apoptotic body formation, suggesting that the compound **6g** induced apoptosis in MCF-7 cancer cells in dose dependent manner.

### Figure 2

### 2.2.3. DAPI nucleic acid staining

DAPI (4',6-diamidino-2-phenylindole), a fluorescent dye capable of strong binding to A–T rich sequences of DNA and helps in the visualization of

chromatin condensation or nuclear damage [31]. It distinguishes live cells from apoptotic cells by staining the characteristic condensed nuclei of the latter bright blue. Therefore, this staining technique was considered of interest to detect the induction of apoptosis by the compound **6g** in MCF-7 cells. The results from **Figure 3** demonstrated that the nuclear structure of untreated control cells was intact whereas cells treated with **6g** displayed condensed, fragmented nuclei.

### Figure 3

#### 2.2.4. Cell cycle analysis

Loss of DNA content is a typical characteristic feature of apoptosis. Treatment with **6g** that blocks cell division led to changes in the frequency of cells in every phase relative to untreated cells. MCF-7 cells were treated with compound **6g**, at concentrations of 1.25, 2.5, 5 and 10  $\mu\text{M}$  for 24 h, and stained with propidium iodide and analysed by using BD FACSVerse™ flow analyser [32]. The results from **Figure 4** indicates that the untreated control cells exposed to DMSO showed 20.53% cells in G2/M phase, whereas compound **6g** treatment resulted in increased G2/M population to 21.01% at 1.25 $\mu\text{M}$ , 22.18% at 2.5 $\mu\text{M}$ , 24.44% at 5 $\mu\text{M}$ , and 26.82% at 10 $\mu\text{M}$  concentration and S phase population from 10.73% in control to 11.76% at 1.25 $\mu\text{M}$ , 12.98% at 2.5 $\mu\text{M}$ , 13.75% at 5 $\mu\text{M}$ , and 15.79% at 10 $\mu\text{M}$  concentration. These results clearly indicated that treatment of MCF-7 cells with the compound **6g** arrest cell growth at G2/M phase and S phase.

### Figure 4

#### 2.2.5. Mitochondrial membrane potential

It is known mitochondria play a pivotal role in apoptosis in response to stress and the loss of mitochondrial membrane potential (MMP) is a sensitive marker of early mitochondrial damage during apoptosis which can be studied by JC1 staining assay [33]. MCF-7 cells upon treatment with compound **6g** at

concentrations of 1.25, 2.5, 5 and 10  $\mu\text{M}$  for 24 hours were stained with JC1 dye and analysed with flow cytometer. **Figure 5** indicated that increase in apoptotic cells (depolarized cell population) from 14.56% in control to 48.95%, 37.15 %, 29.08 % and 28.36% in 10, 5, 2.5 and 1.25 $\mu\text{M}$  indicates decreased mitochondrial membrane potential in dose dependent manner by compound **6g** in MCF-7 cells.

### Figure 5

#### 2.2.6. AnnexinV/Propidium iodide dual staining assay

To quantify the percentage of apoptosis induced by compound **6g** in MCF-7 cells, the Annexin V/Propidium iodide dual staining assay [34] was carried. The Annexin V-Alexa Flour 488/PI dual staining assay facilitates the detection of live cells (LC; AV-/ PI-), early apoptotic cells (EA; AV+/PI-), late apoptotic cells (LA; AV+/PI+) and necrotic cells (NC; AV-/PI+). **Figure 6** shows that MCF-7 cells with compound **6g** displayed rise in total percentage of apoptotic (early and late apoptotic cells-Annexin v + cells) and dead cells from 10.77% in control to 11.43% in 1.25 $\mu\text{M}$ , 12.98% in 2.5 $\mu\text{M}$ , 21.06% in 5 $\mu\text{M}$ , and 36.47% in 10 $\mu\text{M}$  respectively in a dose dependent manner.

### Figure 6

#### 2.2.7. Dichlorofluorescein (DCF) fluorescence

The effect of compound **6g** on cellular Reactive Oxygen Species (ROS) levels in MCF-7 cells was studied using cell permeant fluorogenic dye DCFDA (2',7' – Dichlorofluorescein diacetate) [35]. A significant increase of ROS levels was observed in cells treated with **6g** at concentrations of 1.25, 2.5, 5 and 10 $\mu\text{M}$ . The percentage of ROS generation by compound **6g** in dose dependent manner was confirmed by intensity of DCF as showed in **Figure 7**.

### Figure 7

### 2.2.8. Effect of compound 6g on Gal-1 expression:

Human Gal-1, protein of lectin family showing affinity towards  $\beta$ -galactosides has emerged as a critical regulator of tumor progression and metastasis, by modulating diverse biological events including homotypic cell aggregation, migration, apoptosis, angiogenesis and immune escape. Recent reports demonstrated that knockdown of Gal-1 suppresses the growth and invasion of osteosarcoma cells through inhibition of the MAPK/ERK pathway [36], Immune escape due to the suppression of T-Cells [37], Increasing Heparin-binding epidermal growth factor (HB-EGF) [38]. *Compagno et. al.*, showed importance of glycan and galectins in prostate cancer angiogenesis and metastasis [39]. Compound **6g** was examined for its effect on Gal-1 levels. Briefly, MCF-7 cells were treated with different concentration of compound 6g (10, 30, 100 and 300 $\mu$ M) and after 24hr of treatment, supernatant was collected. Equal amounts of supernatant were subjected to quantitative enzyme immunoassay as per manufacture's protocol [DGAL10, R&D Systems, USA]. Reduced levels of Gal-1 expression by compound **6g** (**Figure 8**) in dose dependent manner was observed. **Table 2** represents the amount of Gal-1 protein expression in control and 6g treated cells. The Gal-1 protein expression by compound **6g** was calculated against standard graph produced as per the supplier's instructions.

**Figure 8**

**Table 2:** Amount of Gal-1 protein expression in control and **6g** treated MCF-7 cells.

concentration	Absorbance at 450 nm	Gal-1 concentration( $\mu$ g/mL)
Control	0.5323	3.337825
6g (10 $\mu$ M)	0.3400	1.550186
6g (30 $\mu$ M)	0.3369	1.521375

6g (100 $\mu$ M)	0.3005	1.183086
6g (300 $\mu$ M)	0.2500	0.713755

### Figure 9

Binding of **6g** to Gal-1 protein was studied by chromatographic analysis using RP-HPLC [40, 41]. Initially the RP-HPLC method was developed for compound **6g** using chromatographic parameters as mentioned in the experimental section, where **6g** showed  $85.44 \pm 0.91\%$  binding efficiency with Gal-1 protein, which indicates there is an existence of the strong interaction of compound **6g** with Gal-1 protein and the chromatographic results were shown in **Figure 9**. These results stipulate that the molecular target of 1-benzyl-1H-benzimidazole derivatives might be Gal-1.

#### 2.2.9. Fluorescence Spectroscopy study

The maximum emission spectra of Gal-1 was at 343 nm and there was decrease in fluorescence intensity with increasing concentration of the compound (**Figure 10A**). The plot of  $\log[6g]$  versus  $\log(F_0-F)/F$  had given a linear relationship (**Figure 10B**) and the number of binding sites were calculated from the slope, which were found to be 1 and infers interaction of protein and

### Figure 10

compound in 1:1 ratio. The binding constant ( $K_a$ ) was calculated from the intercept value which was observed as  $1.2 \times 10^4 \text{ M}^{-1}$ . The intensity of the fluorescence was quenched upon increase of ligand concentration and the bimolar quenching constant ( $K_q$ ) was calculated to be  $2.3 \times 10^{12} \text{ M}^{-1} \text{ S}^{-1}$  which is larger than diffusion control limit [42] suggesting interaction of protein and ligand as well as the mode of quenching to be static.

#### 2.2.10. Surface Plasmon Resonance (SPR) studies

The Gal-1/**6g** interaction was analyzed through SPR using immobilized Gal-1 (ligand, 8070 RU) and compound **6g** (analyte) at various concentrations. Sensorgram was measured for each of concentration of compound **6g** (**Figure 11**) and fitted using 1:1 interaction steady state affinity model. The equilibrium constant  $K_D$  value was found to be  $5.76 \times 10^{-4}$  M using Biacore T200 Evaluation software version 2.0. SPR analysis has shown interaction of Gal-1/**6g**, which is in corroboration with florescence studies.

**Figure 11**

### 2.2.11. Molecular docking

The interaction of Gal-1 with the compound **6g** was studied using molecular docking calculations using the Glide docking module of Schrödinger suite. The 3D crystal co-ordinates of human Gal-1 were retrieved from protein data bank (PDB ID: 1GZW). The ligand interaction diagram of **6g** was shown in **Figure 12**. Hydrogen bonding interaction was found at a distance of  $2.58\text{\AA}$  between phenolic OH acting as a donor (atom no. 20152) and C=O of ASP125 acting as

**Figure 12**

an acceptor (atom no. 950). Additional hydrogen bond was found at a distance of  $4.23\text{\AA}$  between C=NH<sub>2</sub><sup>+</sup> of ARG48 that acts as donor (atom no. 360) and benzimidazole nitrogen acting as an acceptor (atom no. 2028). Further,  $\pi$ -cation interaction was found between nitrogen of ARG48 and aromatic group of **6g** and three  $\pi$ - $\pi$  stacking between indole ring of TRP68 and benzimidazole as well as aromatic ring system of **6g**.

A set of ADMET related properties were calculated using qikprop program (Qikprop, version 6.5, Schrödinger, LLC, New York, NY, 2014). The physicochemical properties of **6g** are marched with the prescribed ranges as represented in **Table 3**. Additionally, the molecular weight (mol. Wt.), hydrogen bond donors (donor HB), hydrogen bond acceptors (accpt HB),

partition coefficient (QPlogPo/w), exhibited acceptable values that followed Lipinski rule of five.

**Table 3:** The ADMET properties of compound **6g**.

S. No	Properties or Descriptors	Recommended Values	Compound <b>6g</b>
1	Molecular weight	130.0 – 725.0	453.927
2	Dipole moment	1.0 – 12.5	2.796
3	Total SASA	300.0 – 1000.0	764.191
4	Molecular Volume	500.0 – 2000.0	1368.395
5	No. of rotatable bonds	0 – 15	5
6	Donor HB	0.0 – 6.0	2
7	Acceptor HB	2.0 – 20.0	4.75
8	QP Polarizability	13.0 – 70.0	50.638
9	QP logP o/w	2.0 – 6.5	5.793
10	QP log BB	-3.0 – 1.2	-0.863
11	QP log HERG	Concern below -5	-7.708
12	Human Oral Absorption	1-3	1
13	Percent Human Oral Absorption	>80% is high	100
14	Rule of Five violations	<25% is low	1
15	No. of metabolites	Maximum of 4	2

From above studies, it is clear that compound **6g** is not toxic and following Lipinski's rule of 5.

### 3. Conclusion

Human Gal-1 plays an essential role in various biological processes including metastasis, tumour progression and host-pathogen interaction. There are many Gal-1 inhibitors reported in literature which are of monovalent- and multivalent-carbohydrate-based inhibitors, peptides- and peptidomimetics. Current work demonstrates synthesis of a series of 1-benzyl-1H-benzimidazole (**6a-6r**) derivatives and anticancer potentials of compound **6g** on MCF-7 cell lines with an IC<sub>50</sub> of 7.01 ± 0.20 μM. It also explains the underlying molecular events

occurring in the presence of compound **6g**. Together, morphological changes such as cell shrinkage, rounding of cell, membrane blebbing, cell cycle arrest at G2/M and S phase, decrease in MMP and increased ROS levels demonstrates the induction of apoptosis by compound **6g**. A dose dependent decrease in Gal-1 protein expression explains Gal-1 mediated apoptosis by compound **6g**. Further binding affinity studies using fluorescence, SPR and RP-HPLC demonstrate the **6g** binding with Gal-1. Molecular docking studies show the binding orientation of **6g** and its interaction with binding site amino acids. Our data provide new light into design and development of non-carbohydrate, non peptidomimetics small molecule Gal-1 inhibitors.

## **4. Materials and Methods**

### **4.1. Chemistry**

All the starting materials, reagents and solvents were purchased from commercial suppliers. Analytical thin layer chromatography (TLC) was performed on MERCK pre-coated silica gel 60-F254 aluminum plates. Visualization of the spots on TLC plates was achieved either by exposure to iodine vapour and UV light. All melting points were recorded on Stuart® SMP30 melting point apparatus and are uncorrected. Column chromatography was performed using silica gel (60-120 mesh) and was eluted with ethyl acetate-hexane. NMR spectra were recorded on Bruker 500 (500 MHz for <sup>1</sup>H-NMR and 125 MHz for <sup>13</sup>C NMR) using CDCl<sub>3</sub> and DMSO as solvents. Chemical shift was reported in parts per million (ppm) with respect to internal standard Tetra Methyl Silane (TMS). Coupling constants were quoted in Hertz (Hz). High Resolution Mass Spectra (HRMS) were obtained on Agilent Q-TOF-Mass Spectrometer 6540-UHD LC/HRMS operating at 70 eV using direct inlet.

#### **4.1.1. Synthetic procedures and spectral data**

#### **4.1.2. Synthesis of N-benzyl-4-chloro-2-nitroaniline (3)**

The 4-chloro-2-nitroaniline (1 eq) was added directly into water (10 mL) followed by added benzyl bromide (1.5 eq) and the reaction mixture was then stirred under reflux at 100 °C for 3-4 hours. After confirmation by TLC the reaction mixture was removed and extracted with ethyl acetate (3x20 ml) and dried over Na<sub>2</sub>SO<sub>4</sub>. The combined organic layer was concentrated in vacuo to give a red colour solid purified by column chromatography.

Red solid, yield 85%; mp 186-188 °C; <sup>1</sup>H NMR (500 MHz, DMSO) δ 8.75 (t, J = 6.0 Hz, 1H), 8.07 (d, J = 2.6 Hz, 1H), 7.50 (dd, J = 9.1, 2.4 Hz, 1H), 7.37 – 7.33 (m, 4H), 7.28 – 7.24 (m, 1H), 6.94 (d, J = 9.3 Hz, 1H), 4.65 (d, J = 6.2 Hz, 2H). <sup>13</sup>C NMR (125 MHz, DMSO) δ 144.24, 138.64, 136.57, 131.68, 129.08, 127.59, 127.33, 125.44, 119.03, 117.49, 46.20.

#### 4.1.3. Synthesis of N<sup>1</sup>-benzyl-4-chlorobenzene-1,2-diamine (4)

Stannous chloride (5 eq) was added to a solution of N-benzyl-4-chloro-2-nitroaniline (3) in ethanol (5 ml) and the reaction mixture was stirred under reflux at 80 °C for 5-6 hours. The reaction mixture was quenched with diluted NaHCO<sub>3</sub> and formed sticky emulsion type solution. It was filtered by suction filtration with celite bed on Buckner funnel to remove precipitate. Finally, the filtrate was extracted with ethyl acetate (3x20 ml) and dried over Na<sub>2</sub>SO<sub>4</sub>. The combined organic layer was concentrated in vacuo to give a purple colour solid purified by column chromatography.

Brown solid, yield 82%; mp 172-174 °C; <sup>1</sup>H NMR (500 MHz, DMSO) δ 7.41 – 7.10 (m, 5H), 6.57 (d, J = 2.4 Hz, 1H), 6.38 (dd, J = 8.4, 2.4 Hz, 1H), 6.27 (d, J = 8.4 Hz, 1H), 4.92 (s, 2H), 4.28 (d, J = 5.8 Hz, 2H). <sup>13</sup>C NMR (125 MHz, DMSO) δ 140.45, 137.51, 134.74, 128.73, 127.64, 127.12, 120.87, 116.56, 113.46, 111.41, 47.33.

#### 4.1.4. Synthesis of 4-formyl-N-substitutedphenylbenzamides (5a-5h)

To a solution of 4-formylbenzoic acid (1 eq) in dimethylformamide (3 mL) was added HATU (1.5 eq) portion wise. The reaction mixture was then stirred at cooled temperature 0 °C for 30 min, furthermore added substituted anilines (1.1 eq) and DIPEA (3 eq) to the reaction mixture and stirred at room temperature for 2 hours. On cooling at room temperature 20-30 mL of cold water was added and stirred for 10 min. The solid separated out was filtered with pump and dried. The products obtained were recrystallized from ethanol.

#### 4.1.5. General procedure for the synthesis of final compounds (6a-6r).

N1-benzyl-4-chlorobenzene-1, 2-diamine (4) (1 eq) was added to water and ethanol mixed solvent (1:1) and to this added sodium metabisulphite (15 eq) and finally added of aromatic, heterocyclic aldehydes and 4-formyl-N-substituted phenyl benzamides (5a-5h) (1 eq). The reaction mixture was stirred under reflux 80 °C for overnight. On cooling at room temperature 20-30 mL of cold water was added and stirred for 10 min. The solid separated out was filtered at pump and dried. The residues were purified by column chromatography on silica gel.

##### 4.1.5.1. 4-(1-benzyl-5-chloro-1H-benzo[d]imidazol-2-yl)-N-phenylbenzamide (6a)

Off white solid, yield 81%; mp 257-259 °C; <sup>1</sup>H NMR (500 MHz, DMSO) δ 10.40 (s, 1H), 8.11 (d, J = 8.3 Hz, 2H), 7.92 (d, J = 8.3 Hz, 2H), 7.86 (d, J = 1.8 Hz, 1H), 7.80 (d, J = 7.8 Hz, 2H), 7.62 (d, J = 8.7 Hz, 1H), 7.39 – 7.25 (m, 6H), 7.12 (t, J = 7.4 Hz, 1H), 7.01 (d, J = 7.3 Hz, 2H), 5.69 (s, 2H). <sup>13</sup>C NMR (125 MHz, DMSO) δ 165.21, 154.19, 143.53, 139.47, 136.93, 136.65, 135.29, 132.62, 129.59, 129.36, 129.12, 128.62, 128.13, 127.58, 126.56, 124.34, 123.81, 120.87, 119.18, 113.29, 48.22. HRMS (ESI): m/z calcd for C<sub>27</sub>H<sub>20</sub>ClN<sub>3</sub>O, 437.1295, found 438.1385 [M+H]<sup>+</sup>.

**4.1.5.2. 4-(1-benzyl-5-chloro-1H-benzo[d]imidazol-2-yl)-N-(methoxyphenyl) benzamide (6b)**

Pale brown solid, yield 80%; mp 206-208 °C; <sup>1</sup>H NMR (500 MHz, DMSO) δ 10.28 (s, 1H), 8.09 (d, J = 8.1 Hz, 2H), 7.91 (d, J = 8.1 Hz, 2H), 7.86 (s, 1H), 7.70 (d, J = 8.7 Hz, 2H), 7.61 (d, J = 8.7 Hz, 1H), 7.38-7.26 (m, 4H), 7.01 (d, J = 7.4 Hz, 2H), 6.94 (d, J = 8.8 Hz, 2H), 5.68 (s, 2H), 3.75 (s, 3H). <sup>13</sup>C NMR (125 MHz, DMSO) δ 164.74, 156.15, 154.26, 143.67, 136.96, 136.69, 135.33, 132.55, 132.52, 129.55, 129.35, 128.50, 128.12, 127.51, 126.56, 123.74, 122.46, 119.22, 114.25, 113.25, 55.66, 48.20. HRMS (ESI): m/z calcd for C<sub>28</sub>H<sub>22</sub>ClN<sub>3</sub>O<sub>2</sub>, 467. 1401, found 468.1492 [M+H]<sup>+</sup>.

**4.1.5.3. 4-(1-benzyl-5-chloro-1H-benzo[d]imidazol-2-yl)-N-(4-isopropyl phenyl) benzamide (6c).**

Off white solid, yield 84%; mp 218-220 °C; <sup>1</sup>H NMR (500 MHz, DMSO) δ 10.39 (s, 1H), 8.10 (d, J = 6.9 Hz, 2H), 7.95 – 7.88 (m, 2H), 7.86 (d, J = 1.6 Hz, 1H), 7.84 – 7.78 (m, 1H), 7.70 (d, J = 7.2 Hz, 1H), 7.61 (d, J = 8.5 Hz, 1H), 7.35 – 7.21 (m, 6H), 7.01 (d, J = 6.2 Hz, 2H), 5.68 (s, 2H), 2.83 (d, J = 38.7 Hz, 1H), 1.20 (d, J = 6.8, 3H), 1.06 (d, J = 7.0, 3H). <sup>13</sup>C NMR (125 MHz, DMSO) δ 165.13, 154.18, 143.57, 136.93, 136.45, 135.30, 132.70, 129.60, 129.35, 128.59, 128.13, 127.57, 126.83, 126.55, 123.80, 122.74, 120.98, 119.19, 115.80, 113.28, 48.21, 33.40, 24.42, 19.02. HRMS (ESI): m/z calcd for C<sub>30</sub>H<sub>26</sub>ClN<sub>3</sub>O, 479. 1764, found 480.1859 [M+H]<sup>+</sup>.

**4.1.5.4. 4-(1-benzyl-5-chloro-1H-benzo[d]imidazol-2-yl)-N-(4-fluorophenyl) benzamide (6d)**

white solid, yield 82%; mp 222-224 °C; <sup>1</sup>H NMR (500 MHz, DMSO) δ 10.43 (s, 1H), 8.09 (d, J = 8.4 Hz, 2H), 7.91 (d, J = 8.4 Hz, 2H), 7.84 (d, J = 1.9 Hz, 1H), 7.83 – 7.79 (m, 2H), 7.60 (d, J = 8.7 Hz, 1H), 7.33 – 7.20 (m, 6H), 7.00 (d, J = 7.2 Hz, 2H), 5.67 (s, 2H). <sup>13</sup>C NMR (125 MHz, DMSO) δ 165.15, 154.31,

144.45, 143.95, 137.01, 135.41, 132.95, 129.57, 129.35, 128.57, 128.11, 127.42, 126.83, 126.53, 123.68, 122.74, 120.97, 119.33, 115.81, 113.20, 48.17. HRMS (ESI):  $m/z$  calcd for  $C_{27}H_{19}ClFN_3O$ , 455. 1201, found 456.1284 [M+H]<sup>+</sup>.

**4.1.5.5. 4-(1-benzyl-5-chloro-1H-benzo[d]imidazol-2-yl)-N-(3,4,5-trimethoxyphenyl) benzamide (6e)**

Off white solid, yield 91%; mp 185-187 °C; <sup>1</sup>H NMR (500 MHz, DMSO)  $\delta$  10.28 (s, 1H), 8.09 (d,  $J = 8.4$  Hz, 2H), 7.91 (d,  $J = 8.5$  Hz, 2H), 7.85 (d,  $J = 1.9$  Hz, 1H), 7.60 (d,  $J = 8.7$  Hz, 1H), 7.34 – 7.24 (m, 6H), 7.00 (d,  $J = 7.2$  Hz, 2H), 5.68 (s, 2H), 3.78 (s, 6H), 3.65 (s, 3H). <sup>13</sup>C NMR (125 MHz, DMSO)  $\delta$  164.96, 154.27, 153.10, 143.95, 137.02, 136.48, 135.60, 135.43, 134.32, 132.91, 129.54, 129.35, 128.48, 128.11, 127.42, 126.54, 123.68, 119.34, 113.19, 98.55, 60.60, 56.22, 48.18. HRMS (ESI):  $m/z$  calcd for  $C_{30}H_{26}ClN_3O_4$ , 527. 1612, found 528.1702 [M+H]<sup>+</sup>.

**4.1.5.6. 4-(1-benzyl-5-chloro-1H-benzo[d]imidazol-2-yl)-N-(3,4,5-trimethylphenyl) benzamide (6f)**

white solid, yield 81%; mp 268-270 °C; <sup>1</sup>H NMR (500 MHz, DMSO)  $\delta$  9.83 (s, 1H), 8.13 (d,  $J = 8.4$  Hz, 2H), 7.91 (d,  $J = 8.4$  Hz, 2H), 7.85 (d,  $J = 1.9$  Hz, 1H), 7.57 (d,  $J = 8.7$  Hz, 1H), 7.33 – 7.26 (m, 4H), 7.01 (d,  $J = 7.3$  Hz, 2H), 6.94 (s, 2H), 5.68 (s, 2H), 2.26 (s, 3H), 2.15 (s, 6H). <sup>13</sup>C NMR (125 MHz, DMSO)  $\delta$  164.82, 154.38, 143.99, 137.04, 136.22, 136.10, 135.71, 135.39, 132.94, 132.80, 129.65, 129.36, 128.82, 128.42, 128.10, 127.40, 126.52, 123.64, 119.34, 113.21, 48.18, 21.01, 18.46. HRMS (ESI):  $m/z$  calcd for  $C_{30}H_{26}ClN_3O$ , 479. 1764, found 480.1853 [M+H]<sup>+</sup>.

**4.1.5.7. 4-(1-benzyl-5-chloro-1H-benzo[d]imidazol-2-yl)-N-(4-hydroxyphenyl) benzamide (6g)**

Pale yellow solid, yield 83%; mp 223-225 °C; <sup>1</sup>H NMR (500 MHz, DMSO) δ 10.27 (s, 1H), 7.98 (d, J = 8.3 Hz, 2H), 7.80 (d, J = 8.3 Hz, 2H), 7.74 – 7.66 (m, 3H), 7.49 (d, J = 8.7 Hz, 1H), 7.26-7.12 (m, 5H), 7.00 (d, J = 6.4 Hz, 1H), 6.89 (d, J = 7.3 Hz, 2H), 5.56 (s, 2H). <sup>13</sup>C NMR (125 MHz, DMSO) δ 165.07, 153.95, 147.23, 143.94, 141.06, 136.93, 135.45, 134.85, 131.00, 130.47, 130.04, 129.34, 128.13, 127.49, 126.61, 123.83, 122.34, 119.42, 114.53, 113.31, 48.20. HRMS (ESI): m/z calcd for C<sub>27</sub>H<sub>20</sub>ClN<sub>3</sub>O<sub>2</sub>, 453. 1244, found 454.1330 [M+H]<sup>+</sup>.

#### 4.1.5.8. 4-(1-benzyl-5-chloro-1H-benzo[d]imidazol-2-yl)-N-(4-chlorophenyl) benzamide (6h)

Off white solid, yield 84%; mp 216-218 °C; <sup>1</sup>H NMR (500 MHz, DMSO) δ 10.32 (s, 1H), 7.97 (d, J = 8.4 Hz, 2H), 7.80 (d, J = 8.4 Hz, 2H), 7.73 – 7.67 (m, 3H), 7.48 (d, J = 8.7 Hz, 1H), 7.22 – 7.08 (m, 6H), 6.88 (d, J = 7.2 Hz, 2H), 5.56 (s, 2H). <sup>13</sup>C NMR (125 MHz, DMSO) δ 164.92, 153.90, 143.24, 139.17, 136.63, 136.36, 135.00, 132.32, 129.29, 129.06, 128.83, 128.32, 127.84, 127.28, 126.27, 124.04, 123.51, 120.58, 118.88, 113.00, 47.92. HRMS (ESI): m/z calcd for C<sub>27</sub>H<sub>19</sub>Cl<sub>2</sub>N<sub>3</sub>O, 471. 0905, found 472.0977 [M+H]<sup>+</sup>.

#### 4.1.5.9. 1-benzyl-5-chloro-2-(1H-indol-3-yl)-1H-benzo[d]imidazole (6i)

white solid, yield 85%; mp 247-249 °C; <sup>1</sup>H NMR (500 MHz, CDCl<sub>3</sub>) δ 10.52 (s, 1H), 8.05 (s, 1H), 7.87 (d, J = 7.1 Hz, 1H), 7.46 (d, J = 8.1 Hz, 1H), 7.40-7.34 (m, 3H), 7.30 (d, J = 5.9 Hz, 1H), 7.16 (dd, J = 8.5, 2.6 Hz, 2H), 7.05 (dd, J = 16.4, 8.9 Hz, 2H), 6.98 (d, J = 7.1 Hz, 2H), 5.44 (s, 2H). <sup>13</sup>C NMR (125 MHz, CDCl<sub>3</sub>) δ 151.16, 136.14, 135.99, 135.78, 133.92, 129.25, 128.54, 128.03, 126.23, 125.87, 123.35, 123.28, 123.20, 121.38, 120.60, 118.44, 111.79, 111.05, 48.37. HRMS (ESI): m/z calcd for C<sub>22</sub>H<sub>16</sub>ClN<sub>3</sub>, 357. 1033, found 358.1114 [M+H]<sup>+</sup>.

**4.1.5.10. 1-benzyl-5-chloro-2-(1H-pyrrol-2-yl)-1H-benzo[d]imidazole (6j)**

Off white solid, yield 83%; mp 192-194 °C; <sup>1</sup>H NMR (500 MHz, CDCl<sub>3</sub>) δ 11.22 (s, 1H), 7.71 (d, J = 1.6 Hz, 1H), 7.40-7.33 (m, 3H), 7.21 – 7.13 (m, 4H), 7.09 (d, J = 0.9 Hz, 1H), 6.56 (s, 1H), 6.29 (dd, J = 6.1, 2.5 Hz, 1H), 5.62 (s, 2H). <sup>13</sup>C NMR (125 MHz, CDCl<sub>3</sub>) δ 148.36, 142.35, 135.28, 134.41, 129.28, 128.74, 128.06, 125.88, 123.17, 122.70, 119.93, 117.98, 111.44, 110.59, 110.56, 48.43. HRMS (ESI): m/z calcd for C<sub>18</sub>H<sub>14</sub>ClN<sub>3</sub>, 307. 0876, found 308.0956 [M+H] +.

**4.1.5.11. 2-(benzo[d] [1,3] dioxol-5-yl)-1-benzyl-5-chloro-1H-benzo[d]imidazole (6k)**

white solid, yield 85%; mp 168-170 °C; <sup>1</sup>H NMR (500 MHz, CDCl<sub>3</sub>) δ 7.89 (s, 1H), 7.38 – 7.32 (m, 3H), 7.25 – 7.19 (m, 3H), 7.12 (d, J = 8.6 Hz, 1H), 7.07 (d, J = 6.6 Hz, 2H), 6.91 – 6.88 (m, 1H), 6.04 (s, 2H), 5.48 (s, 2H). <sup>13</sup>C NMR (125 MHz, CDCl<sub>3</sub>) δ 154.51, 149.77, 148.24, 135.51, 135.43, 134.18, 129.28, 128.91, 128.16, 125.86, 123.96, 123.87, 122.10, 119.14, 111.48, 109.57, 108.82, 101.76, 48.72. HRMS (ESI): m/z calcd for C<sub>21</sub>H<sub>15</sub>ClN<sub>2</sub>O<sub>2</sub>, 362. 0822, found 363.0908 [M+H] +.

**4.1.5.12. 1-benzyl-5-chloro-2-(furan-2-yl)-1H-benzo[d]imidazole (6l)**

Pale yellow solid, yield 82%; mp 164-166 °C; <sup>1</sup>H NMR (500 MHz, CDCl<sub>3</sub>) δ 7.84 (s, 1H), 7.61 (d, J = 1.1 Hz, 1H), 7.35-7.24 (m, 4H), 7.25 – 7.19 (m, 2H), 7.12 (d, J = 6.7 Hz, 2H), 6.60 (dd, J = 3.5, 1.7 Hz, 1H), 5.72 (s, 2H). <sup>13</sup>C NMR (125 MHz, CDCl<sub>3</sub>) δ 145.02, 144.77, 144.15, 142.83, 135.66, 134.04, 129.08, 128.07, 126.23, 124.05, 119.22, 114.41, 112.32, 111.00, 48.70. HRMS (ESI): m/z calcd for C<sub>18</sub>H<sub>13</sub>ClN<sub>2</sub>O, 308. 0716, found 309.0799 [M+H] +.

**4.1.5.13. 1-benzyl-5-chloro-2-(pyridin-2-yl)-1H-benzo[d]imidazole (6m)**

Off white solid, yield 84%; mp 140-142 °C; <sup>1</sup>H NMR (500 MHz, CDCl<sub>3</sub>) δ 8.66 (d, J = 4.3 Hz, 1H), 8.57 (d, J = 7.5 Hz, 1H), 7.95 – 7.88 (m, 2H), 7.39 (dd, J = 6.9, 4.9 Hz, 1H), 7.30 – 7.26 (m, 3H), 7.26 – 7.22 (m, 2H), 7.16 – 7.13 (m, 2H), 6.22 (s, 2H). <sup>13</sup>C NMR (125 MHz, CDCl<sub>3</sub>) δ 148.90, 137.45, 137.28, 136.58, 134.80, 129.23, 129.20, 128.78, 127.74, 126.76, 125.36, 124.77, 124.66, 119.31, 111.87, 49.31. HRMS (ESI): m/z calcd for C<sub>19</sub>H<sub>14</sub>ClN<sub>3</sub>, 319. 0876, found 320.0957 [M+H] +.

**4.1.5.14. 1-benzyl-5-chloro-2-(thiophen-2-yl)-1H-benzo[d]imidazole (6n)**

white solid, yield 83%; mp 178-180 °C; <sup>1</sup>H NMR (500 MHz, CDCl<sub>3</sub>) δ 7.87 (s, 1H), 7.54 (d, J = 5.0 Hz, 1H), 7.47 (s, 1H), 7.39 – 7.30 (m, 3H), 7.23 (d, J = 8.6 Hz, 1H), 7.17 (d, J = 8.6 Hz, 1H), 7.11 (dd, J = 12.5, 6.1 Hz, 3H), 5.61 (s, 2H). <sup>13</sup>C NMR (125 MHz, CDCl<sub>3</sub>) δ 149.00, 135.37, 134.66, 129.63, 129.41, 129.30, 129.13, 128.90, 128.25, 128.15, 125.89, 125.79, 123.94, 119.35, 110.92, 48.47. HRMS (ESI): m/z calcd for C<sub>18</sub>H<sub>13</sub>ClN<sub>2</sub>S, 324. 0488, found 325.0568 [M+H] +.

**4.1.5.15. 2-(1-benzyl-5-chloro-1H-benzo[d]imidazol-2-yl) quinolin-8-ol (6o)**

Yellow solid, yield 85%; mp 292-294 °C; <sup>1</sup>H NMR (500 MHz, CDCl<sub>3</sub>) δ 8.45 (d, J = 8.6 Hz, 1H), 8.25 (d, J = 8.7 Hz, 1H), 7.87 (s, 1H), 7.44 – 7.24 (m, 6H), 7.19 (s, 1H), 7.15 (d, J = 7.3 Hz, 2H), 7.02 (d, J = 7.6 Hz, 1H), 6.91 (s, 1H), 5.95 (s, 2H). <sup>13</sup>C NMR (125 MHz, CDCl<sub>3</sub>) δ 152.72, 137.70, 137.55, 137.34, 135.48, 130.81, 130.10, 129.59, 127.79, 127.43, 124.91, 124.84, 124.76, 122.94, 122.16, 120.00, 113.35, 112.61, 49.93. HRMS (ESI): m/z calcd for C<sub>23</sub>H<sub>16</sub>ClN<sub>3</sub>O, 385. 0982, found 386.1060 [M+H] +.

**4.1.5.16. 1-benzyl-5-chloro-2-(3-phenoxyphenyl)-1H-benzo[d]imidazole (6p)**

Off white solid, yield 82%; mp 176-178 °C;  $^1\text{H}$  NMR (500 MHz, DMSO)  $\delta$  7.80 (d,  $J = 1.3$  Hz, 1H), 7.58 – 7.52 (m, 2H), 7.49 (d,  $J = 7.6$  Hz, 1H), 7.40 (t,  $J = 7.8$  Hz, 2H), 7.34 – 7.27 (m, 4H), 7.23 – 7.14 (m, 3H), 7.04 (d,  $J = 7.9$  Hz, 2H), 6.95 (d,  $J = 6.7$  Hz, 2H), 5.60 (s, 2H).  $^{13}\text{C}$  NMR (125 MHz, DMSO)  $\delta$  157.63, 156.51, 154.32, 143.67, 136.90, 135.26, 131.74, 131.14, 130.64, 129.56, 129.29, 128.03, 127.35, 126.49, 124.48, 124.29, 123.54, 120.67, 119.53, 119.20, 119.08, 113.09, 48.16. HRMS (ESI):  $m/z$  calcd for  $\text{C}_{26}\text{H}_{19}\text{ClN}_2\text{O}$ , 410. 1186, found 411.1270  $[\text{M}+\text{H}]^+$ .

**4.1.5.17. 4-(1-benzyl-5-chloro-1H-benzo[d]imidazol-2-yl)-2-ethoxyphenol (6q)**

white solid, yield 91%; mp 147-149 °C;  $^1\text{H}$  NMR (500 MHz, DMSO)  $\delta$  9.64 (s, 1H), 7.78 (d,  $J = 1.9$  Hz, 1H), 7.53 (d,  $J = 8.6$  Hz, 1H), 7.35 – 7.26 (m, 4H), 7.20 – 7.17 (m, 2H), 7.04 (d,  $J = 7.3$  Hz, 2H), 6.93 (d,  $J = 8.7$  Hz, 1H), 5.62 (s, 2H), 3.97 (q,  $J = 8.2$  Hz, 2H), 1.26 (t,  $J = 7.0$  Hz, 3H).  $^{13}\text{C}$  NMR (125 MHz, DMSO)  $\delta$  155.39, 149.41, 147.16, 137.24, 135.24, 129.60, 129.33, 127.99, 127.26, 126.45, 123.09, 122.68, 120.31, 118.54, 116.25, 114.46, 112.82, 64.21, 48.24, 15.03. HRMS (ESI):  $m/z$  calcd for  $\text{C}_{22}\text{H}_{19}\text{ClN}_2\text{O}_2$ , 378. 1135, found 379.1225  $[\text{M}+\text{H}]^+$ .

**4.1.5.18. 4-(1-benzyl-5-chloro-1H-benzo[d]imidazol-2-yl)-2,6-dimethoxyphenol (6r)**

Off white solid, yield 91%; mp 208-210 °C;  $^1\text{H}$  NMR (500 MHz, DMSO)  $\delta$  9.01 (s, 1H), 7.79 (s, 1H), 7.54 (d,  $J = 8.5$  Hz, 1H), 7.37 – 7.23 (m, 4H), 7.07 (d,  $J = 7.2$  Hz, 2H), 6.92 (s, 2H), 5.63 (s, 2H), 3.65 (s, 6H).  $^{13}\text{C}$  NMR (126 MHz, DMSO)  $\delta$  155.53, 148.40, 143.68, 138.07, 137.52, 135.58, 129.35, 127.94, 127.14, 126.37, 123.05, 119.48, 118.75, 112.65, 107.00, 56.29, 48.29. HRMS (ESI):  $m/z$  calcd for  $\text{C}_{22}\text{H}_{19}\text{ClN}_2\text{O}_2$ , 394. 1084, found 395.1171  $[\text{M}+\text{H}]^+$ .

**4.2. Biology**

#### 4.2.1. Cell culture

Lung cancer (A-549), prostate cancer (DU-145), Breast cancer (MCF-7), Breast cancer (MDA-MB-231), Colorectal cancer (HCT-116), Colorectal cancer (HT-29) cell lines were procured from National Centre for Cell Science, Pune, India. All the cell lines were grown in appropriate DMEM, MEM and RPMI-1640 medium (Sigma-Aldrich, USA). Cells were supplemented with 10% fetal bovine serum stabilized with 1% antibiotic-antimycotic solution (Sigma-Aldrich, USA) in a CO<sub>2</sub> incubator at 37 °C in incubator. When the cells reached up to 80-90% of confluency, they were sub-cultured using 0.25% trypsin/1 mM EDTA solution for further passage.

#### 4.2.2. MTT assay

This MTT assay is a colorimetric assay that measures the reduction of 3-(4,5-dimethylthiazol-2-yl)-2,5-diphenyl tetrazolium bromide (MTT) by mitochondrial succinate dehydrogenase. The MTT enters the cells and passes into the mitochondria where it gets reduced and forms insoluble dark purple formazan crystals. The crystals are then solubilized with an organic solvent DMSO and the soluble formazan product is measured by reading absorbance at 570 nm with spectrophotometer (Spectra Max, M4 Molecular devices, USA). Since reduction of MTT can only occur in metabolically active cells, the level of activity is the measure of the viability of the cells. Briefly, cells were seeded in 96-well plates at a density of 10<sup>3</sup> cells per well in 100 µl of complete medium and allowed to grow overnight for attachment. Then the cells were treated with various concentrations of the compounds for a period of 48 hrs. After the treatment, 100 µl of MTT (0.5 mg/ml) was added and incubated at 37 °C for 4 h. Then MTT reagent was aspirated and the formazan crystals formed were dissolved by the addition of 200 µL of DMSO for 20 mins at 37 °C. The quantity of formazan product was measured by using a spectrophotometric microtiter plate reader at 570 nm wavelength. Initially, cytotoxicity effects of

the synthetic derivatives were screened by MTT assay at 50  $\mu\text{M}$  concentration. Among these, the compound which shown  $\text{IC}_{50}$  value  $<20 \mu\text{M}$  was used for the dose dependent studies at various concentrations ranging from 1.56  $\mu\text{M}$  to 100  $\mu\text{M}$  in serial dilutions and the percentage of cytotoxicity was calculated.

#### **4.2.3. Acridine orange/ethidium bromide (AO/EB) staining**

MCF-7 cells were treated with 1.25, 2.5, 5 and 10  $\mu\text{M}$  of compound 6g. Plates were incubated in an atmosphere of 5%  $\text{CO}_2$  at 37  $^\circ\text{C}$  for 48 h, followed by addition of fluorescent dyes containing AO/EB into each well in equal volumes and within 10 min cells were visualized under fluorescence microscope (Nikon, Inc. Japan) with excitation (488 nm) and emission (550 nm) at 200X magnification.

#### **4.2.4. DAPI staining**

MCF-7 cells were cultured in 12-well plates and treated with 1.25, 2.5, 5 and 10  $\mu\text{M}$  of compound 6g. The untreated and treated cells were washed two times with PBS, followed by fixation with 4% paraformaldehyde and staining with 10  $\mu\text{g}/\text{mL}$  of DAPI. The cells were observed for apoptotic characteristics under fluorescence microscope (Nikon, Inc. Japan) with excitation at 359 nm and emission at 461 nm using DAPI filter at 200X magnification.

#### **4.2.5. Cell cycle analysis**

MCF-7 ( $1 \times 10^6$  cells/well) in 6 well plate was treated with 1.25, 2.5, 5 and 10  $\mu\text{M}$  of compound 6g for 24 h. Cells were collected by trypsinisation, washed with PBS and fixed with 70% ethanol for 30 min at 4 $^\circ\text{C}$ . After fixing, cells were washed with PBS and stained with 400  $\mu\text{L}$  of propidium iodide staining buffer for 30 min in dark at room temperature. The samples were then analysed for propidium iodide fluorescence from 10,000 events by flow cytometry using BD Accuri C6 flow cytometer.

#### 4.2.6. Assay of mitochondrial membrane potential ( $\Delta\psi_m$ ):

The mitochondrial-specific cationic dye JC-1 (Invitrogen, USA), which undergoes potential-dependent accumulation in mitochondria, was used to detect mitochondrial membrane potential. Briefly, cells were plated at a seeding density of  $2 \times 10^5$  cells/well in a 12-well plate. After 48 h of treatment with 6g (1.25, 2.5, 5 and 10  $\mu\text{M}$ ), cells were incubated with 2  $\mu\text{M}$  JC-1 for 30 min at room temperature in the dark and the quantitative analysis of  $\Delta\psi_m$  was done by flow cytometry.

#### 4.2.7. Annexin V/Propidium iodide dual staining assay

The Annexin V/Propidium iodide dual staining assay was performed by using MCF-7 cells, to quantify the percentage of apoptotic cells. Cells were plated in 12-well culture plates and allowed to grow for 24 h. After treatment with 1.25, 2.5, 5 and 10  $\mu\text{M}$  of compound 6g for 48 h, cells were collected by trypsinisation. The collected cells were washed twice with ice-cold PBS, then incubated with 200  $\mu\text{L}$  1X binding buffer containing 5  $\mu\text{L}$  Annexin V-FITC, and then in 300  $\mu\text{L}$  1X binding buffer containing 5  $\mu\text{L}$  Propidium iodide (PI) in the dark for 5 min at room temperature and incubate for 15 min. After 15 min of incubation, cells were analysed for percentage of apoptosis using BD-C6 accurate flow-cytometer.

#### 4.2.8. Detection of intracellular ROS

Intracellular ROS generation was measured by DCF-DA method. MCF-7 cells were seeded into a 12-well plate and allowed to grow for 24 h. After treatment with 1.25, 2.5, 5 and 10  $\mu\text{M}$  of 6g for 48 h, then cells were incubated with 10  $\mu\text{M}$  DCF-DA at 37°C for 15 min. The intracellular reactive oxygen species (ROS) mediated oxidation of DCFDA to the fluorescent compound 2,7-dichlorofluorescein (DCF) monitored by excitation (498 nm) and emission (530 nm) using Multimode Plate Reader (Spectra Max M4, Molecular devices,

USA). The images were taken by fluorescence microscope at 200X magnification.

#### **4.2.9. Statistical analysis**

All the values were expressed as mean  $\pm$  SEM. The intergroup variation between different groups was measured by one-way ANOVA using the Graph Pad Prism, version 6.01. Here, the results were considered statistically significant when \* $p < 0.05$ .

#### **4.2.10. Quantikine ELISA Human Gal-1 Immunoassay**

This assay employs the quantitative sandwich enzyme immunoassay technique. A polyclonal antibody specific for human Gal-1 has precoated on a microplate. Standards and samples are pipetted into the wells and Gal-1 present is bound by the immobilized antibody. After washing away any unbound substances, an enzyme-linked polyclonal antibody specific for human Gal-1 is added to the wells. Following a wash to remove any unbound antibody-enzyme reagent, a substrate solution is added to the wells and colour develops in proportion to the amount of Gal-1 bound in the initial step. The colour development is stopped and the intensity of the colour is measured at 450 nm in a multi detection plate reader (Spectramax M4, molecular devices, USA). MCF-7 cells were seeded in petri dish and allowed to attached for 24hr after that cells were treated with different concentration of compound 6g (10, 30, 100 and 300 $\mu$ M) and after 24hr of treatment cells supernatant was collected and cell lysis collected by adding cell lysis buffer (RIPA) and cells are sonicated. The galectin quantikine ELISA was done by using R & D human galectins quantikine ELISA kit.

##### **4.2.10.1 Determination of binding efficiency of compound 6g with RP-HPLC**

The assay for **6g** was carried out by high-performance liquid chromatography (HPLC). The analysis was carried out by automatic RP-HPLC (Waters Corp,

USA) on X-bridge C18 column (250 mm X 4.6 mm, 5  $\mu$ m) with a mobile phase consisted of ammonium acetate (pH 6.3) and Acetonitrile (v/v). The mobile phase was filtered through 0.22  $\mu$ m membrane filter, sonicated and used. The analysis was performed in gradient mode at a flow rate of 1 ml/min with 210 nm as detection wavelength and the injection volume of 20  $\mu$ l. The HPLC sample was prepared by using amicon Ultra-4 centrifugal filters containing an Ultracel 10k regenerated cellulose membrane (10,000 MW cut-off), were purchased from Millipore, USA. Before addition of compound **6g**, each of these filtration devices was filled with 1 ml of PBS. The membrane was washed by spinning the filtration device at 10000 x g for 1 min. Compound **6g** was incubated with Gal-1 for 30 min at 37  $^{\circ}$ C to allow the binding interactions. Immediately, after PBS washing, 0.5  $\mu$ g/ml concentration of compound **6g** (control) or compound **6g** with Gal-1 protein (0.5  $\mu$ g / ml concentration) sample was introduced into centrifugal filters. These devices were spun in the centrifugal filters at 7500 x g and 25  $^{\circ}$ C for 30 min. The filtrates were collected and their contents were analysed by RP-HPLC as per the chromatographic conditions. In each case, ultrafiltration units were pre-treated with compound **6g** and washed with PBS several times to avoid non-specific binding and to ensure complete removal of compound **6g** from units before subjecting to actual test samples. The binding efficiency is calculated by the following formula.

$$\% \text{ Gal-1 binding efficiency} = (\text{Bound drug concentration} / \text{Free drug concentration}) \times 100$$

#### **4.2.10.2 Chromatographic conditions**

Chromatographic analysis was performed on Alliance HPLC system e 2695 separation module equipped (Waters Corp., Milford, M.A, USA) with an in-line degasser, quaternary pump, an autosampler, a column compartment with temperature control facility and a photo diode array detector (model 2998). The

output signal was monitored and processed using Waters Empower 3 software (Waters Corp.).

Mobile phase: Ammonium acetate (pH 6.3) (solvent A): Acetonitrile (solvent B), Diluent: Acetonitrile, Column: X-bridge C18 column (250 mm X 4.6 mm, 5  $\mu$ m), Lambda max ( $\lambda_{\text{max}}$ ): 299 nm, Flow rate: 1 ml/min, Injection volume: 20  $\mu$ l

#### Optimized method

Time (min)	% A	% B
0.00	90	10
2.00	90	10
6.00	10	90
11.00	10	90
12.00	90	10
13.00	90	10

#### 4.2.10.3. Fluorescence measurements

In order to perform fluorescence binding studies of Gal-1 with compound **6g**, full length ORF of Gal-1 was cloned into pET28a expression vector followed by purification using Ni-NTA affinity chromatography as reported by Hsieh and co-authors, 2015. Intrinsic fluorescence measurements were carried out on a Jasco spectrofluorimeter equipped with peltier at 25 °C. Compound **6g** was dissolved in DMSO to prepare a stock of 10 mM and was used in the range of 0-65  $\mu$ M. Purified Gal-1 with concentration of 13  $\mu$ M in 10 mM phosphate buffer (pH 7.5) was excited at 280 nm and the emission was recorded from 300-400 nm using a cuvette of 10 mm path length. Slit width 5 nm was used for excitation and emission, while scan speed was maintained at 100 nm/min. Buffer correction was made for each spectra. Binding constant ( $K_a$ ) and number of binding sites ( $n$ ) were determined using modified Stern-Volmer equation i.e.  $\log(F_0-F)/F = \log K_a + n \log [Q]$  where  $F_0$  and  $F$  is the intensity of

the protein in the absence and presence of the ligand respectively, whereas  $n$  is the number of binding sites and  $Q$  is the ligand concentration.

#### 4.2.10.4. Surface Plasmon Resonance (SPR) study

The binding of Gal-1 with compound **6g** was studied by surface plasmon resonance using Biacore T200 instrument. Gal-1 was immobilized on a series S CM5 sensor chip at 100 $\mu$ g/ml concentration in 10 mM sodium acetate pH 5.0 using standard amine coupling method. The compound **6g** was serially diluted in running buffer (PBS + 0.05% P20 + 2% DMSO) and introduced onto immobilized Gal-1 surface for 60 sec at a flow rate of 30  $\mu$ l/min. Subsequently, the sensor chip was regenerated with 50% DMSO at the end of each cycle and the solvent correction was done using the standard protocol for small molecule assays in Biacore system.

#### 4.2.11. Molecular modelling studies

All computational calculations were carried out on an Intel (R) Xenon(R) 2 Duo CPU E7600 @ 3.06GHz processor with the LINUX operating system. Software package used was the Schrodinger drug discovery consisting of modules for protein and, ligand preparation and Glide for high-throughput virtual screening for docking. Protein preparation wizard was used to prepare Gal-1 downloaded from PDB (PDB ID: 1GZW), ready for docking i.e. removing waters, adding missing side chains and energy minimization by OPLS-2005 force field. The final compound **6g** was sketched and converted to 3D using Ligprep. The Glide XP docking algorithm was employed using a grid box volume of 10x 10x 10 Å.

#### Acknowledgements

Authors are thankful to Department of Biotechnology (DBT), Govt. of India, New Delhi, for the young investigators in cancer biology start up grants (6242-19/RGCB/PMD/DBT/MLKA/2015).

## References

- 1 I. Camby, M. Le Mercier, F. Lefranc and R. Kiss, Galectin-1: a small protein with major functions, *Glycobiology*. 16 (2006) 137R-157R.
- 2 J. Ellerhorst, T. Nguyen, D. N. Cooper, D. Lotan and R. Lotan, Differential expression of endogenous galectin-1 and galectin-3 in human prostate cancer cell lines and effects of overexpressing galectin-1 on cell phenotype, *Int. J. Oncol.* 14 (1999) 217–224.
- 3 F. van den Brûle, S. Califice, F. Garnier, P. L. Fernandez, A. Berchuck and V. Castronovo, Galectin-1 accumulation in the ovary carcinoma peritumoral stroma is induced by ovary carcinoma cells and affects both cancer cell proliferation and adhesion to laminin-1 and fibronectin, *Lab. Invest.* 83 (2003) 377–386.
- 4 a) N. Tinari, I. Kuwabara, M.E. Huflejt, P.F. Shen, S. Iacobelli, F.T. Liu, Glycoprotein 90K/MAC-2BP interacts with galectin-1 and mediates galectin-1-induced cell aggregation, *Int. J. Cancer.* 91 (2001) 167–172. b) G.A. Rabinovich, Galectin-1 as a potential cancer target, *Br. J. Cancer.* 92 (2005) 1188–1192.
- 5 F. A. van den Brûle, C. Buicu, M. Baldet, M. E. Sobel, D. N. Cooper, P. Marschal and V. Castronovo, Castronovo, Galectin-1 modulates human melanoma cell adhesion to laminin, *Biochem. Biophys. Res. Commun.* 209 (1995) 760–767.
- 6 S. Rorive, N. Belot, C. Decaestecker, F. Lefranc, L. Gordower, S. Micik, C. A. Maurage, H. Kaltner, M. M. Ruchoux, A. Danguy, H. J. Gabius, I. Salmon, R. Kiss and I. Camby, Galectin-1 is highly expressed in human gliomas with relevance for modulation of invasion of tumor astrocytes into the brain parenchyma, *Glia.* 33 (2001) 241–255.

- 7 N. L. Perillo, K. E. Pace, J. J. Seilhamer and L. G. Baum, Apoptosis of T cells mediated by Galectin-1, *Nature*. 378 (1995) 736–739.
- 8 P. Matarrese, A. Tinari, E. Mormone, G. A. Bianco, M. A. Toscano, B. Ascione, G. A. Rabinovich and W. Malorni, Galectin-1 sensitizes resting human T lymphocytes to Fas (CD95)-mediated cell death via mitochondrial hyperpolarization, budding and fission, *J. Biol. Chem.* 280 (2005) 6969–6985.
- 9 C. Fischer, H. Sanchez-Ruderisch, M. Welzel, B. Wiedenmann, T. Sakai, S. André, H.-J. Gabius, L. Khachigian, K. M. Detjen and S. Rosewicz, Galectin-1 interacts with the  $\alpha 5\beta 1$  fibronectin receptor to restrict carcinoma cell growth via induction of p21 and p27, *J. Biol. Chem.* 280 (2005)
- 10 S. André, H. Kaltner, M. Lensch, R. Russwurm, H.-C. Siebert, C. Fallsehr, E. Tajkhorshid, A. J. R. Heck, M. von Knebel Doeberitz, H.-J. Gabius and J. Kopitz, Determination of structural and functional overlap/divergence of five proto-type galectins by analysis of the growth-regulatory interaction with ganglioside GM1 in silico and in vitro on human neuroblastoma cells, *Int. J. Cancer*. 114 (2005) 46–57.
- 11 G. Elad-Sfadia, R. Haklai, E. Ballan, H.-J. Gabius and Y. Kloog, Galectin-1 augments Ras activation and diverts Ras signals to Raf-1 at the expense of phosphoinositide 3-kinase, *J. Biol. Chem.*, 2002, 277, 37169–37175.
- 12 a) R. Grützmann, C. Pilarsky, O. Ammerpohl, J. Lüttges, A. Böhme, B. Sipos, M. Foerder, I. Alldinger, B. Jahnke, H. K. Schackert, H. Kalthoff, B. Kremer, G. Klöppel and H. D. Saeger, Gene expression profiling of microdissected pancreatic ductal carcinomas using high-density DNA microarrays, *Neoplasia*. 6 (2004) 611–622. b) J. Shen, M. D. Person, J. Zhu, J. L. Abbruzzese and D. Li, Protein expression profiles in pancreatic adenocarcinoma compared with normal pancreatic tissue and tissue affected by

pancreatitis as detected by two-dimensional gel electrophoresis and mass spectrometry, *Cancer Res.* 64 (2004) 9018–9026.

13. H. Blanchard, K. Bum-Erdene, M.H. Bohari, X. Yu, Galectin-1 inhibitors and their potential therapeutic applications: a patent review, *Expert Opinion on Therapeutic Patents.* 26 (2016) 537–554.

14 K. Kubo, Y. Inada, Y. Kohara, Y. Sugiura, M. Ojima, K. Itoh, Y. Furukawa, K. Nishikawa and T. Naka, Nonpeptide angiotensin II receptor antagonists. Synthesis and biological activity of benzimidazoles, *Journal of Medicinal Chemistry.* 36 (1993) 1772–1784.

15 M. Sabat, J. C. VanRens, M. J. Laufersweiler, T. A. Brugel, J. Maier, A. Golebiowski, B. De, V. Easwaran, L. C. Hsieh, R. L. Walter, M. J. Mekel, A. Evdokimov and M. J. Janusz, the development of 2- benzimidazole substituted pyrimidine based inhibitors of lymphocyte specific kinase (Lck), *Bioorganic & Medicinal Chemistry Letters.* 16 (2006) 5973–5977.

16 Ö. Ö. Güven, T. Erdoğan, H. Göker and S. Yıldız, Synthesis and antimicrobial activity of some novel phenyl and benzimidazole substituted benzyl ethers, *Bioorganic & Medicinal Chemistry Letters.* 17 (2007) 2233–2236.

17 L. B. Townsend, R. V. Devivar, S. R. Turk, M. R. Nassiri and J. C. Drach, Design, Synthesis, and Antiviral Activity of Certain 2,5,6-Trihalo-1-( $\beta$ -D-ribofuranosyl) benzimidazoles, *Journal of Medicinal Chemistry.* 38 (1995) 4098–4105.

18 J. Valdez, R. Cedillo, A. Hernández-Campos, L. Yépez, F. Hernández-Luis, G. Navarrete-Vázquez, A. Tapia, R. Cortés, M. Hernández and R. Castillo, Synthesis and antiparasitic activity of 1H-benzimidazole derivatives, *Bioorganic & Medicinal Chemistry Letters.* 12 (2002) 2221–2224.

- 19 C. Kuş, G. Ayhan-Kılıcıgil, S. Özbey, F. B. Kaynak, M. Kaya, T. Çoban and B. Can-Eke, Synthesis and antioxidant properties of novel N-methyl-1,3,4-thiadiazol-2-amine and 4-methyl-2H-1,2,4-triazole-3(4H)- thione derivatives of benzimidazole class, *Bioorganic & Medicinal Chemistry*. 16 (2008) 4294–4303.
- 20 Z. Zhao, D. O. Arnaiz, B. Griedel, S. Sakata, J. L. Dallas, M. Whitlow, L. Trinh, J. Post, A. Liang, M. M. Morrissey and K. J. Shaw, Design, synthesis, and in vitro biological activity of benzimidazole based factor Xa inhibitors, *Bioorganic & Medicinal Chemistry Letters*. 10 (2000) 963–966.
- 21 S. Selvakumar, I. Sudheer Babu and N. Chidambaranathan, In-vivo Central Nervous System- Locomotor Activity of Some Synthesized 2- [(1-((phenyl amino) methyl) Substituted 1-benzoimidazol-2-yl) alkyl] Isoindoline-1, 3-diones, *Biosciences Biotechnology Research Asia*. 10 (2013) 937–943.
- 22 W. G. Schulz, I. Islam and E. B. Skibo, Pyrrolo[1,2-a] benzimidazole-Based Quinones and Iminoquinones. The Role of the 3-Substituent on Cytotoxicity, *Journal of Medicinal Chemistry*. 38 (1995) 109–118.
- 23 M. Matsuyama, K. Funao, K. Kuratsukuri, T. Tanaka, Y. Kawahito, H. Sano, J. Chargui, J.-L. Touraine, N. Yoshimura and R. Yoshimura, Telmisartan inhibits human urological cancer cell growth through early apoptosis, *Exp Ther Med*. 1 (2010) 301–306.
- 24 T.-C. Shih, R. Liu, G. Fung, G. Bhardwaj, P.M. Ghosh, K.S. Lam, A Novel Galectin-1 Inhibitor Discovered through One-Bead Two-Compound Library Potentiates the Antitumor Effects of Paclitaxel in vivo, *Molecular Cancer Therapeutics*. 16 (2017) 1212–1223.
- 25 T.-C. Shih, R. Liu, C.-T. Wu, X. Li, W. Xiao, X. Deng, S. Kiss, T. Wang, X.-J. Chen, R. Carney, H.-J. Kung, Y. Duan, P.M. Ghosh, K.S. Lam, Targeting Galectin-1 Impairs Castration-Resistant Prostate Cancer Progression and Invasion, *Clinical Cancer Research*. 24 (2018) 4319–4331.

- 26 D. N. Kommi, D. Kumar, R. Bansal, R. Chebolu and A. K. Chakraborti, "All-water" chemistry of tandem N-alkylation–reduction–condensation for synthesis of N-arylmethyl-2-substituted benzimidazoles, *Green Chemistry*. 14 (2012) 3329.
- 27 J. M. Humphrey and A. R. Chamberlin, Chemical Synthesis of Natural Product Peptides: Coupling Methods for the Incorporation of Noncoded Amino Acids into Peptides, *Chemical Reviews*. 97 (1997) 2243–2266.
- 28 S. I. Alaqeel, Synthetic approaches to benzimidazoles from o-phenylene diamine: A literature review, *Journal of Saudi Chemical Society*. 21 (2017) 229–237.
- 29 V. Naidu, U. M. Bandari, A. K. Giddam, K. R. D. Babu, J. Ding, K. S. Babu, B. Ramesh, R. R. Pragada and P. Gopalakrishna, Apoptogenic activity of ethyl acetate extract of leaves of *Memecylon edule* on human gastric carcinoma cells via mitochondrial dependent pathway, *Asian Pacific Journal of Tropical Medicine*. 6 (2013) 337–345.
- 30 S. Shrivastava, P. Kulkarni, D. Thummuri, M. K. Jeengar, V. G. M. Naidu, M. Alvala, G. B. Reddy and S. Ramakrishna, Piperlongumine, an alkaloid causes inhibition of PI3 K/Akt/mTOR signaling axis to induce caspase-dependent apoptosis in human triple-negative breast cancer cells, *Apoptosis*. 19 (2014), 1148–1164.
- 31 B. I. Tarnowski, F. G. Spinale and J. H. Nicholson, DAPI as a useful stain for nuclear quantitation, *Biotech Histochem*. 66 (1991) 297–302.
- 32 U. V. Mallavadhani, C. V. Prasad, S. Shrivastava and V. G. M. Naidu, Synthesis and anticancer activity of some novel 5,6-fused hybrids of juglone based 1,4-naphthoquinones, *European Journal of Medicinal Chemistry*. 83 (2014) 84–91.

33 N. Kulabaş, E. Tatar, Ö. Bingöl Özakpınar, D. Özsavcı, C. Pannecouque, E. De Clercq and İ. Küçükgül, Synthesis and antiproliferative evaluation of novel 2-(4 H -1,2,4-triazole-3-ylthio) acetamide derivatives as inducers of apoptosis in cancer cells, *European Journal of Medicinal Chemistry*. 121 (2016) 58–70.

34 C. Praveen Kumar, T. S. Reddy, P. S. Mainkar, V. Bansal, R. Shukla, S. Chandrasekhar and H. M. Hügel, Synthesis and biological evaluation of 5,10-dihydro-11 H -dibenzo[ b,e ][1,4]diazepin-11-one structural derivatives as anti-cancer and apoptosis inducing agents, *European Journal of Medicinal Chemistry*. 108 (2016), 674–686.

35 S. Marchi, C. Giorgi, J. M. Suski, C. Agnoletto, A. Bononi, M. Bonora, E. De Marchi, S. Missiroli, S. Patergnani, F. Poletti, A. Rimessi, J. Duszynski, M. R. Wieckowski and P. Pinton, Mitochondria-ros crosstalk in the control of cell death and aging, *J Signal Transduct*. 2012 (2012) 329635.

36 J.-H. Miao, S.-Q. Wang, M.-H. Zhang, F.-B. Yu, L. Zhang, Z.-X. Yu and Y. Kuang, Knockdown of Galectin-1 suppresses the growth and invasion of osteosarcoma cells through inhibition of the MAPK/ERK pathway, *Oncology Reports*. 32 (2014) 1497–1504.

37 T. Dalotto-Moreno, D. O. Croci, J. P. Cerliani, V. C. Martinez-Allo, S. Dergan-Dylon, S. P. Mendez-Huergo, J. C. Stupirski, D. Mazal, E. Osinaga, M. A. Toscano, V. Sundblad, G. A. Rabinovich and M. Salatino, Targeting Galectin-1 Overcomes Breast Cancer-Associated Immunosuppression and Prevents Metastatic Disease, *Cancer Research*. 73 (2013) 1107–1117.

38 P.-L. Kuo, M.-S. Huang, D.-E. Cheng, J.-Y. Hung, C.-J. Yang and S.-H. Chou, Lung Cancer-derived Galectin-1 Enhances Tumorigenic Potentiation of Tumor-associated Dendritic Cells by Expressing Heparin-binding EGF-like Growth Factor, *Journal of Biological Chemistry*. 287 (2012) 9753–9764.

39 D. Compagno, L. D. Gentilini, F. M. Jaworski, I. G. Perez, G. Contrufo and D. J. Laderach, Glycans and galectins in prostate cancer biology, angiogenesis and metastasis, *Glycobiology*. 24 (2014) 899–906.

40 S. Doppalapudi, A. Jain, D.K. Chopra, W. Khan, Psoralen loaded liposomal nanocarriers for improved skin penetration and efficacy of topical PUVA in psoriasis, *European Journal of Pharmaceutical Sciences*. 96 (2017) 515–529

41 A.E. Pires, N.K. Honda, C.A.L. Cardoso, A method for fast determination of psoralens in oral solutions of phytomedicines using liquid chromatography, *Journal of Pharmaceutical and Biomedical Analysis*. 36 (2004) 415–420.

42. Joseph R. Lakowicz, *Principles of Fluorescence Spectroscopy*, third edition, Springer, 2006.

## Synthesis of 1-benzyl-1H-benzimidazoles as galectin-1 mediated anticancer agents

Nerella Sridhar Goud <sup>a</sup>, S. Mahammad. Ghouse <sup>a</sup>, Jatoth Vishnu <sup>b</sup>, D. Komal <sup>a</sup>, Venu Talla <sup>b</sup>, Ravi Alvala <sup>c</sup>, Jakkula Pranay <sup>d</sup>, Janish Kumar <sup>d</sup>, Insaf A. Qureshi <sup>d</sup>, Mallika Alvala <sup>a\*</sup>

<sup>a</sup> Department of Medicinal Chemistry, National Institute of Pharmaceutical Education and Research (NIPER), Hyderabad 500 037, India

<sup>b</sup> Department of Pharmacology and Toxicology, National Institute of Pharmaceutical Education and Research (NIPER), Hyderabad 500 037, India

<sup>c</sup> G. Pulla Reddy College of Pharmacy, Hyderabad 500 028, India.

<sup>d</sup> School of life sciences, University of Hyderabad, Hyderabad 500 046, India

